British Journal of Pharmaceutical Research
13(3): 1-14, 2016, Article no.BJPR.29357
ISSN: 2231-2919, NLM ID: 101631759

SCIENCEDOMAIN *international*
www.sciencedomain.org

Adsorption Kinetics and Equilibrium of Ciprofloxacin from Aqueous Solutions Using *Corylus avellana* (Hazelnut) Activated Carbon

Davoud Balarak[1], Ferdos Kord Mostafapour[1] and Hossein Azarpira[2*]

[1]Department of Environmental Health, Health Promotion Research Center, School of Public Health, Zahedan University of Medical Sciences, Zahedan, Iran.
[2]Department of Environmental Health, Faculty of Health School, Saveh University of Medical Sciences, Saveh, Iran.

Authors' contributions

This work was carried out in collaboration between all authors. All authors read and approved the final manuscript.

Article Information

DOI: 10.9734/BJPR/2016/29357
Editor(s):
(1) Wenbin Zeng, School of Pharmaceutical Sciences, Central South University, Hunan, China.
Reviewers:
(1) Lorna T. Enerva, Polytechnic University of the Philippines, Philippines.
(2) M. Mupa, Bindura University of Science Education, Zimbabwe.
Complete Peer review History: http://www.sciencedomain.org/review-history/16334

Original Research Article

Received 6th September 2016
Accepted 21st September 2016
Published 26th September 2016

ABSTRACT

The adsorption of Ciprofloxacin (CIP) from aqueous solutions by hazelnut shell activated carbon (HSAC) was studied in a batch adsorption system. Factors influencing CIP adsorption such as contact time (10-180 min), initial CIP concentration (25–200 mg/L), pH (3–11), adsorbent dosage (0.3–3.0 g/L) and temperature (293–323 K) were investigated. The adsorption process was relatively fast and equilibrium was established about 60 min. Maximum adsorption of CIP occurred at around pH 6. A comparison of the kinetic models on the overall adsorption rate showed that the adsorption system was best described by the pseudo second-order kinetics. The adsorption equilibrium data fitted best with the Langmuir isotherm and the monolayer adsorption capacity of CIP was determined as 61.25, 67.39, 73.64 mg/g at 273, 298 and 323 K, respectively. Thermodynamic parameters were calculated for the CIP–HSAC system and the positive value of ΔH^0 (3.064 kJ/mol) and negative values of ΔG^0 showed that the adsorption was endothermic, spontaneous and physical in nature.

**Corresponding author: E-mail: H.azarpira@savehums.ac.ir;*

Keywords: Hazelnut shell; activated carbon; ciprofloxacin; adsorption kinetics; adsorption equilibrium; thermodynamics.

1. INTRODUCTION

Environmental problems, including water, air and soil pollution and climate change, have attracted more global attention in the last century [1,2]. Pharmaceuticals are released to the environment through many ways, including municipal medical and industrial wastewater effluents [3]. They are extremely resistant to biological degradation processes and because of their continuous discharge, they remain in the environment for a long time; their presence in the environment has caused increased concern over long-term effect on human health [4].

Ciprofloxacin (CIP) is a synthetic fluoroquinolone antibiotics that are amphoteric due to consists of a bicyclic aromatic ring skeleton with a carboxylic acid group (pKa = 6.1), a keto group, and a basic- N -moiety (pKa=8.89) which was selected to represent a group of antibiotics in this study, is also one of the most frequently detected fluoroquinolone antibiotics in the wastewater plant effluent and in surface and ground waters [5-7]. CIP is an important bacteriostatic agentthatis commonly used in human and veterinary medicine. The release of CIP in to the ecosystem or wastewater effluents has caused pollution and many human diseases [8].

The most commonly used methods for the removal of antibiotics from aqueous solution are liquid membrane separation, Adsorption, bioaugmentation, electro-Fenton oxidation, nanofiltration, sono-chemical degradation, enzymatic complexation [9]. Most of these methods suffer from some drawbacks, such as high capital and operational cost or the disposal of the residual sludge, and are not suitable for small-scale industries [10-12].

Adsorption is an effective and versatile method for removing antibiotics. Natural materials that are available in large quantities, or certain waste products from industrial or agricultural operations, may have potential as inexpensive sorbents [13]. Due to their low cost, after these materials have been expended, they can be disposed of without expensive regeneration [14]. Most of the low cost sorbents have the limitation of low sorptive capacity and thereby for the same degree of treatment, it generates more solid waste (pollutant laden sorbent after treatment), which poses disposal problems. Therefore, there is need to explore low cost sorbent having high contaminant sorption capacity [15-17].

Many reports have appeared on the development of low cost activated carbon from cheaper and readily available materials. Activated carbons, with their high surface area, micro porous character and chemical nature of their surface, have made them potential adsorbents for the removal of antibiotics from industrial wastewater [18-20].

In this study, hazelnut shell (*Corylus avellana*) was utilized as the raw material for the production of granular activated carbon and its adsorption capacity for CIP from aqueous solutions was evaluated. Effects of initial CIP concentration, contact time, pH, adsorbent dosage and temperature on hazelnut shell activated carbon (HSAC) under kinetic and equilibrium conditions were investigated. Thermodynamic parameters were also calculated.

2. MATERIALS AND METHODS

Ciprofloxacin (CIP) (formula mass 367.8 g/mol) with purity higher than 99.6% was supplied by Sigma–Aldrich. Its pKa_1 and pKa_2 values are 6.1 and 8.7. The chemical molecular formulae and structure of the CIP are $C_{17}H_{18}FN_3O_3$ is given in Fig. 1. 1000 mg/L of CIP stock solution was prepared by dissolving the required amount of CIP in distilled water. Other concentrations of CIP were obtained by dilution of the stock solution. Solution pH was adjusted using NaOH and HNO_3 purchased from Fluka. All reagents used in this study were analytical grade purchased from Merck Co., Germany and were used without any further purification.

Hazelnut shell, for the synthesis of AC was collected from a local source in the north of Iran. Fresh hazelnut shells were washed several times with distilled water to remove surface impurities, dried at 100 ℃ overnight, crushed by a hammer mill and sieved to a particle size of 251–354 nm. For the production of AC, hazelnut shell (5 g) was mixed to 40 mL of $ZnCl_2$ solution at 1–1 impregnation ratio (defined by the weight ratio of $ZnCl_2$ to hazelnut shell) and was stirred for 6 h. The mixture was dried in an oven at 105℃ for 24 h to ensure a complete reaction between $ZnCl_2$ and hazelnut shell. Then the mixtures were

filtered and the residual solids were dried at 120 ℃ for about 48 h in an oven to remove extra water. The dried impregnated hazelnut shell was placed in an inert atmosphere in a vertical furnace as used in our previous works at 650℃ for 1 h under the nitrogen flow of 300 mL/min at heating rate of 10℃ 1/min. The resulting AC was thoroughly washed with 0.05 M HCl and distilled water to remove the residual $ZnCl_2$ and inorganic material until the pH value of the washed solution reached neutral value (between 6 and 7). Afterwards, the granular activated carbon was washed three times with distilled water, dried at 110 ℃ for 24 h and stored in a desiccator. The yield of prepared hazelnut shell AC was calculated based on the following equation [21]:

$$Y\ (\%) = W_{AC}/W \times 100 \quad (1)$$

where W_{AC} and W are the weights of carbon product, and dried pods.

2.1 Structure Characterization of HSAC

The surface properties of the synthesized materials were calculated by the nitrogen adsorption–desorption isotherm at 77 K using volumetric adsorption analyzer apparatus (Micromeritics, USA, ASAP 2020). The morphologies and mesoporous pore structure of HSAC were observed by a scanning electron microscope (SEM, JEOL, JEOL-6700F).

2.2 A Batch Mode Adsorption Studies

The effects of experimental parameters such as, initial CIP concentration (25–200 mg/L), pH (3–11), adsorbent dosage (0.3–3.0 g/L) and temperature (273–323 K) on the adsorptive removal of CIP were studied in a batch mode of operation for a specific period of contact time (0–180 min). The CIP solutions were prepared by dissolving 1 g in distilled water and used as a stock solution (1000 mg/L) and diluted to the required initial concentration. pH was adjusted using 0.1M HCl and NaOH. For kinetic studies, 50 mL of CIP solution of known initial concentration and initial pH was taken in a 250 mL screw-cap conical flask with a fixed adsorbent dosage (1.5 g/L) and was agitated in a thermostated rotary shaker for a contact time varied in the range 0–180 min at a speed of 200 rpm at 293 K. At various time intervals, the adsorbent was separated from the samples by filtering and the filtrate was analysed using a HPLC model Knauer. The analytical column was an C18 column (150 mm× 4.6 mm). HPLC column operated at ambient temperature, UV wavelength was set at 277 nm. A 20:80 (v/v) methanol and phosphate buffer mixture was used as mobile phase at room temperature with a constant flow rate of 0.7 mL min^{-1}.

The amount of CIP adsorbed onto AC and removal efficiency (R) was calculated by equations 2 and 3, respectively [22]:

$$q_e = \frac{(Co-Ce)\times V}{M} \quad (2)$$

$$R = \frac{(Co-Ce)}{C_0} \times 100 \quad (3)$$

Where C_0 and C_e (mg/L) are the initial and equilibrium concentrations of CIP, respectively. V (L) is the volume of the solution and W (g) is the mass of adsorbent.

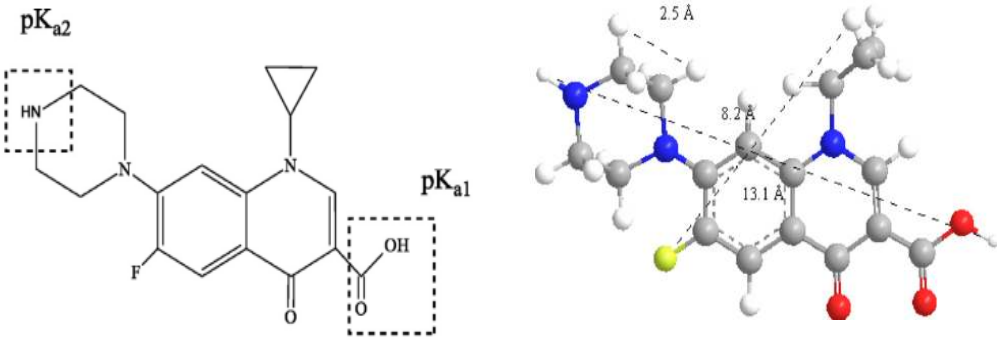

Fig. 1. Chemical molecular formulae and structure of CIP (The molecular dimensions size of L13.1°A × W8.2°A × H2.5◦°A)

2.3 Determination of Point of Zero Charge (pH_{pzc})

The pH_{pzc} characteristics of the hazelnut shell AC were determined using the solid addition method. For this purpose, 25 mL of 0.2 M KNO_3 solution was prepared in different flasks. Their pH was roughly adjusted between 2 and 12 by adding either 0.2 M HCl. The total volume of the solution in each flask was exactly adjusted to 50 mL by adding KNO_3 solution of the same strength. The pH of the solutions was accurately noted. Next, 0.5 g of HSAC was added to each flask and the suspensions were placed in a shaker for 24 h and allowed to equilibrate for 1 h. The final pH values (pH_f) of the supernatant liquid were noted.

3. RESULTS AND DISCUSSION

In this study, we attempted to identity adsorption properties of HSAC as the adsorbentsfor CIP from synthetic solutions. The characteristics of HSAC are summarized in Table 1. It is clearly seen from Table 1 that the Prepared HSAC had a specific surface area of 1247.2 m^2/g, total pore volume of 0.515 cm^3/g, a porosity of 58% and an bulk density of 0.723 g/cm^3. The Scanning electron microscopy (SEM) of prepared HSAC before and after adsorption indicated in Fig. 2. As it can be observed from Fig. 2, the pores of the adsorbent after adsorption, filled with CIP molecules. Also SEM showed that carbon texture and development of porosity was strongly affected by characteristics of the starting materials. Carbons obtained from Hazelnut shells had an homogeneous structure with a predominance of macropores with an average 12 μm diameter.

As shown in Fig. 3, pH_{pzc} for HSAC was obtained at 6.5. In this regard, HSAC at pH values less and more than 6.5 demonstrates cationic and anionic behavior, respectively. The pH_{pzc} can be used to determine the quality of the relation between pH and CIP adsorption value.

3.1 Effect of pH

The highest adsorption of CIP onto the HSAC occurred at a pH of about 6 which was near the pKa value of CIP and thereafter the adsorption process started to decrease as pH exceeds 6. Optimum pH of 6 was selected for further studies (Fig. 4). Electrostatic interaction plays a significant role in CIP sorption. Its acid dissociation constants pK_{a1} and pK_{a2} for CIP in cation state and in anion state were 6.1 and 8.7, respectively [7]. The positively charged form of the molecule was dominant due to the protonation of the amine group at pH below 6.1. The zwitterionic species of CIP molecules dominate in the aqueous solution because of deprotonating the carboxylic group to the negatively charged carboxylate as this pH range is higher than pK_{a1} of the carboxylic group and the amine group stays protonated and positively charged as this pH range is still lower than pK_{a2} of the amine group at pH between 6.1 and 8.7. The negatively charged form of CIP dominated due to the loss of a proton from the carboxylic group at pH above 8.7.

Also sorption capacity of adsorbents is largely dependent on the ionization or surface charge state. At $pH<pH_{pzc}$, the surface of all the adsorbents are presented positively charged, and the CIP^+ should be the dominant species in the aqueous solutions, favoring the adsorption process due to electrostatic attraction between the adsorbent and adsorbate [23,24[. The CIP molecules exist in a zwitterionic or neutral zwitterionic form at pH value of 6.1~8.7. A slight decrease in the adsorption amount of CIP on HSAC in a zwitterionic or neutral form was observed. This result can due to the fact that there is no significant electrostatic attraction or repulsive between the CIP and charged surface ions for the adsorption sites [25]. When pH was greater than 8.7, CIP stay negatively charged in aqueous solution, a drastic decrease in CIP sorption amount was observed (Fig. 4), which could be attributed to the electrostatic repulsion between the negatively charged HSAC surfaces and the CIP molecules. Therefore, electrostatic interaction between HSAC and CIP molecules should be the major factor controlling the sorption process.

3.2 Adsorbent Dose Effect

The contents of adsorbent were between 0.3 and 3 g/L. Fig. 5 shows the uptake of CIP by HSAC at various adsorbent doses. The removal percentage increased with an increase in the adsorbent dose. Thus a tendency was originally ascribed with enhancement in the adsorbent content of adsorptive surface area enhancement which purveys a higher number of active sites for removal [26-28]. The obtained results can be well explained from the facts that with the increase of adsorbent dosage to the proper amount, active sites of the adsorbent surface increase and more number of CIP molecules can be adsorbed on the surface of CIP- HSAC.

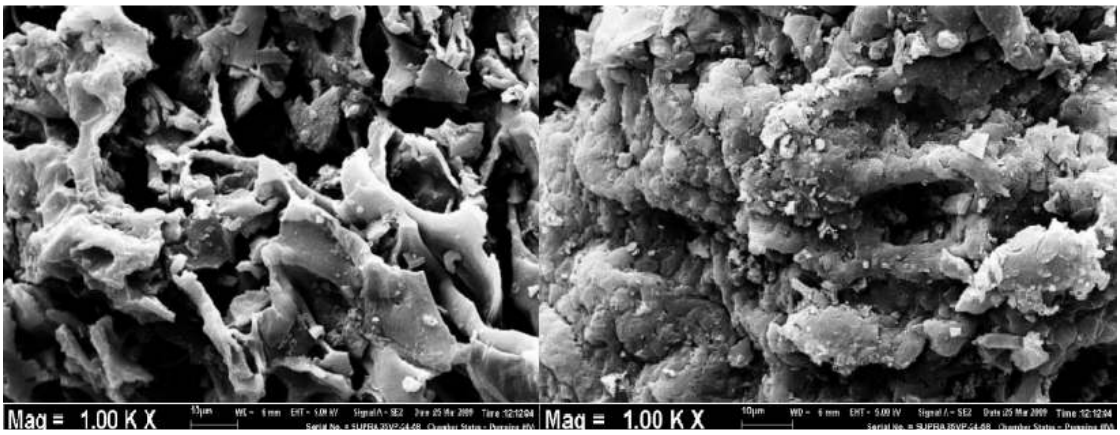

Fig. 2. SEM image of the HSAC adsorbent before (a) and after (b) adsorption

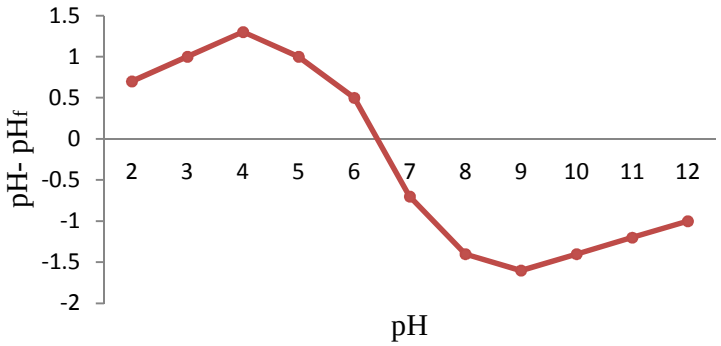

Fig. 3. Determination of the point of zero charges of HSAC

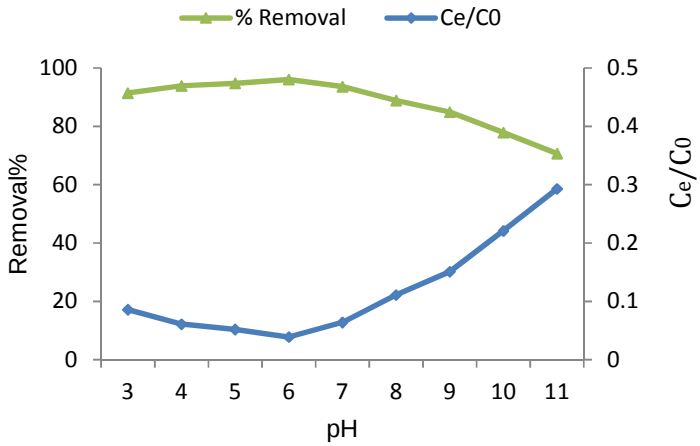

Fig. 4. Effect of pH on CIP removal efficiency (C_0 = 50 mg/L, dose of 1.5 g/L, time= 60 min Temp= 30 ℃)

3.3 Adsorption Kinetics

Fig. 6 describes the variation of adsorption amount with adsorption time at different temperatures. The obtained curves reflect that the adsorption amount increases until equilibrium is attained around 60 min.

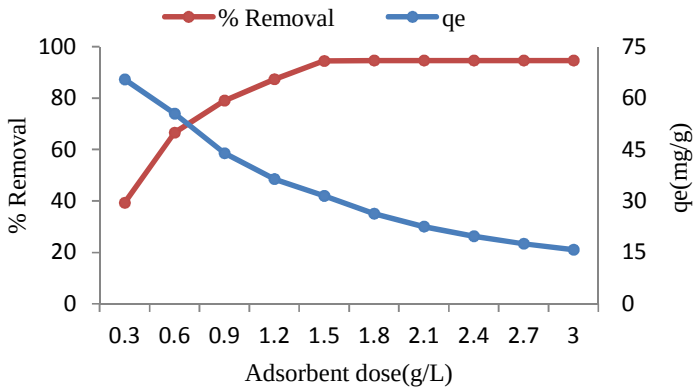

Fig. 5. Effect of adsorbent dose (C_0= 100 mg/L, pH = 6, Contact time 60 min and Temp= 25 ℃)

The adsorption rate is an important parameter used to predict the adsorption process of tested adsorbents in order to design an adsorption treatment plant. The kinetic data of CIP adsorption have been tested by the pseudo-first-order, pseudo-second-order and intraparticle diffusion models using the following equations, respectively.

3.3.1 Pseudo-first-order model

The pseudo-first-order equation is given as equation 4 [29]:

$$\text{Log } (q_e - q_t) = \log q_e - \frac{K_1}{2.303}t \quad (4)$$

Where q_e and q_t are the amount of CIP Adsorbed on the sorbent (mg/g) at equilibrium and at time t, respectively, and k_1 is the rate constant of the first-order adsorption (min^{-1}). The values k_1 for CIP adsorption on HSAC were determined from the plot of log (q_e−q_t) against t.

3.3.2 Pseudo-second-order model

The pseudo-second-order model is represented as equation 5 [30]:

$$\frac{t}{q_t} = \frac{1}{k_2 qe^2} + \frac{t}{qe} \quad (5)$$

Where q_e and q_t are the amounts of CIP adsorbed (mg/g) at equilibrium and at time t (min), respectively, k_2 (g/mg min) are pseudo-second-order rate constants. The linear plot of t/q_t versus t (Fig. 7) for pseudo-second-order model shows the high values of R^2 (Table 2). Moreover, the theoretical adsorption capacity values were in agreement with the experimental adsorption capacity values for this model.

The second-order rate constants were used to calculate the initial sorption rate h (mg/g min) given by [31]:

$$h = k_2 q_2^2 \quad (6)$$

The batch kinetic data were fitted to both first-pseudo and second-pseudo order models. Both models adequately described the kinetic data at 95% confidence level. The results of the kinetic parameters and the calculated initial sorption rate values are listed in Table 2. Based on the correlation coefficients the adsorption of CIP is best described by the pseudo-second-order model and the initial adsorption rate increased with the increase of temperature in a given adsorption system. Several studies which were conducted to remove the antibiotics by adsorbents confirmed the results of this study [13-17]. Furthermore, Table 2 illustrates that the rate constants k_2 increase with increasing temperature, which reveals the fact that it is faster for an adsorption system with SMZ at higher temperature to reach equilibrium. This trend is compatible with those observed for other adsorption systems [14,17].

3.4 Intraparticle Diffusion Kinetic Model

To identify the importance of diffusion in the sorption process, regression analysis was carried out for the graph plotted between the amount of metal sorbed (q) and the square root of time ($t^{1/2}$). The mathematical expression of Weber–Morris kinetic model can be represented as follows equation 7 [32-34]:

$$q_t = K\, t^{1/2} + C \quad (7)$$

K is the rate constant for intra-particle diffusion. Values of C give an idea about the thickness of

the boundary layer, i.e., the larger the intercept, the greater the boundary layer effect will be. According to above equation, a plot of q_t versus $t^{1/2}$ should be linear, if intra-particle diffusion is involved in the adsorption process and if these lines pass through the origin, then intraparticle diffusion is the rate controlling step. Otherwise, the intraparticle diffusion is not the only rate-controlling step but some degree of the boundary layer diffusion (or external mass transfer) also controls the adsorption. Plots of q_t against $t^{1/2}$ are shown in Fig. 8. Fig. 8 shows the three different stages proceed by surface sorption, intra-particle diffusion and a likely chemical reaction stage. The last step from mentioning three steps is very fast and considered negligible. The values of k and C for three stages were obtained through fitting the experimental data with intra-particle equation and were summarized in Table 2. The driving force of diffusion in the adsorption processes, is very important. The regression of q_t versus $t^{1/2}$ for CIP was linear and did not pass through the origin, shows that the boundary layer diffusion control in the adsorption process. Given the large C values of all kinetic studies indicates that the intra-particle diffusion was involved in the adsorption process, however, is not the sole rate-limiting step.

3.4.1 Boyd plot

It is clear that the sorption of CIP on HSAC are complex processes involving external mass transfer and intraparticle diffusion in the rate limiting step of the sorption. However, it was unclear as to which one exerted a greater influence on the rate of CIP sorption. This point was resolved using the Boyd plot. The Boyd plot is obtained by plotting Bt versus time t. The Bt is expressed by the equation 8 [35,36]:

$$Bt = -\ln\left(1 - \frac{q_t}{q_e}\right) - 0.4977 \quad (8)$$

Where q_t and q_e are the amounts of CIP adsorbed on HSAC (mg/g) at time t (min) and at equilibrium time (min), respectively. The calculated Bt values were plotted against time t as shown in Fig. 9. The linearity of the plots will provide useful information to distinguish between external mass transfer and intraparticle diffusion controlled mechanism of adsorption. If the plot passing through the origin implies that intraparticle diffusion controls the rate of mass transfer. The plots in Fig. 8 did not pass through the origin, confirming the involvement of external mass transfer in the entire adsorption process. This result again confirmed the rate-controlling mechanism of adsorption stated in Weber–Morris Kinetic model studies. So both the intraparticle diffusion and the boundary layer diffusion may play an important role in the given adsorption system.

3.5 Adsorption Isotherm

Adsorption isotherms are useful for understanding the mechanism of the adsorption [37]. Although several isotherm equations are available due to their simplicity, three well-known models, Langmuir, Freundlich and Dubinin–Radushkevich (D–R) isotherm models were chosen in this study for evaluating the relationship between the amount of CIP adsorbed onto HSAC and its equilibrium concentration in aqueous solution.

The Langmuir model assumes that adsorption takes place at specific homogeneous sites on the surface of the adsorbent and also, when a site is occupied by an adsorbate molecule, no further adsorption can take place at this site [38]. The linear form of the Langmuir isotherm model can be presented by equation 9 [39]:

$$\frac{C_e}{q_e} = \frac{C_e}{q_{max}} + \frac{1}{q_{max}\, K_L} \quad (9)$$

Where q_e (mg/g) is the amount of the CIP adsorbed per unit mass of adsorbent, Ce (mg/L) is the equilibrium CIP concentration in the solution, q_{max} (mg/g) is the Langmuir constant related to the maximum monolayer adsorption capacity, and K_L (L/mg) is the constant related the free energy or net enthalpy of adsorption. The linear plot of C_e/q_e versus C_e indicates that adsorption obeys the Langmuir model, and the constants q_{max} and K_L are obtained from the slope and intercept of the linear plot, respectively.

The essential features of the Langmuir isotherm model can be expressed in terms of 'R_L' a dimensionless constant, separation factor or equilibrium parameter, which is defined by the equation 10 [40]:

$$R_L = \frac{1}{1 + C_0 K_L} \quad (10)$$

Where C_o (mg/L) is the initial amount of adsorbate and K_L (L/mg) is the Langmuir

constant described above. The R_L parameter is considered as more reliable indicator of the adsorption. There are four probabilities for the R_L value:

For favorable adsorption $0<R_L<1$,
For unfavorable adsorption $R_L>1$,
For linear adsorption $R_L=1$ and
For irreversible adsorption $R_L= 0$

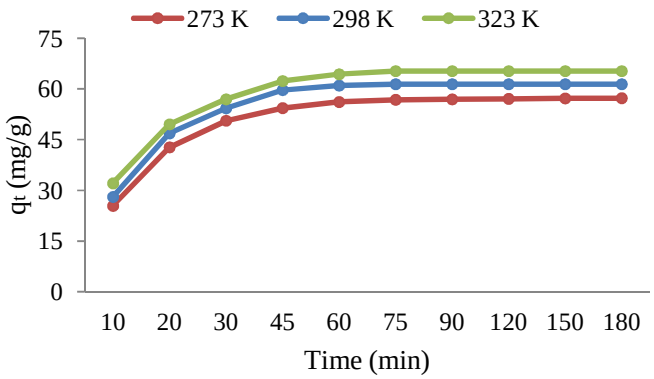

Fig. 6. The effect of temperatures on adsorption capacity (Dose = 2.5 g/L, C_0 = 100 mg/L, pH = 6)

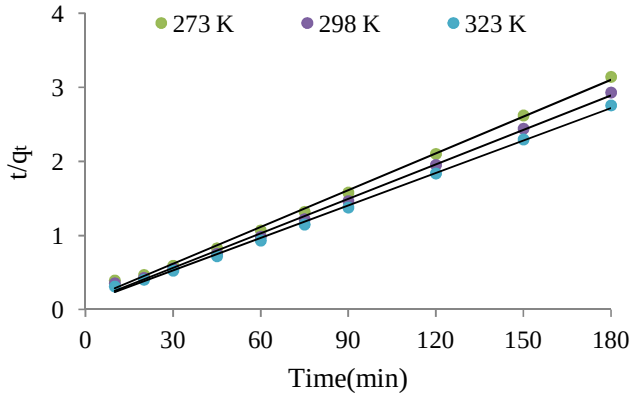

Fig. 7. Pseudo-second-order model plot of IP adsorption on HSAC

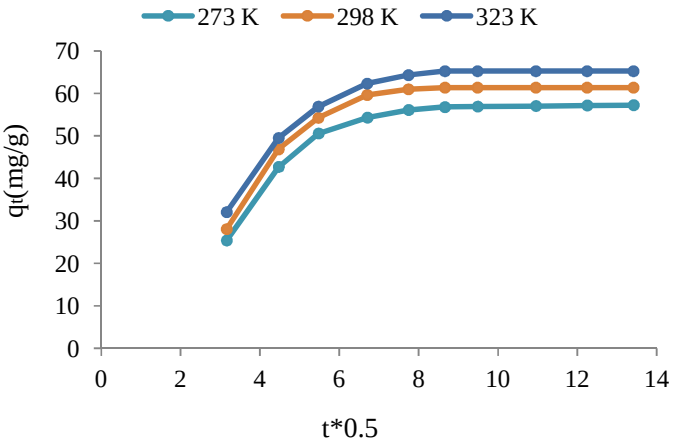

Fig. 8. Intraparticle diffusion plot of IP adsorption on HSAC

Table 1. Important properties of the activated carbons obtained from hazelnut shell

Specific surface area	Average pore diameter	Porosity	pore volume	Moisture	Bulk density	pH	C %	H%	N%	O%	Y	%Ash
1247.2 m^2/g	38.5 nm	58%	0.515 cm^3/g	1.98%	0.723 g/cm^3	7.25	49.6%	4.74%	0.481	41.84	46.6%	2.25

Table 2. Kinetic parameters for the adsorption of CIP onto HSAC at various temperatures

T(K)	$q_e$exp	Pseudo-first order			Pseudo-second order			Intraparticle diffusion								
								Stage 1			Stage 2			Stage 3		
		K_1	q_e	R^2	K_2	q_e	R^2	K_1	C	R^2	K_2	C	R^2	K_3	C	R^2
273	57.26	0.476	44.65	0.952	0.029	55.21	0.998	11.68	1.65	0.912	5.25	8.46	0.972	1.15	12.25	0.954
298	61.25	0.344	47.34	0.961	0.034	59.48	0.997	14.25	2.46	0.924	7.46	9.72	0.956	1.52	14.86	0.936
323	65.44	0.259	51.29	0.947	0.038	64.17	0.999	18.11	3.72	0.908	8.59	11.2	0.947	1.96	15.95	0.941

Table 3. Adsorption isotherm constants for the adsorption of CIP onto HSAC at various temperatures

Temp (°K)	$q_e$exp	Langmuir model				Freundlich model			D–R model		
		q_m (mg/g)	K_L	R_L	R^2	1/n	K_F	R^2	q_m	E	R^2
273	57.26	61.25	0.152	0.061	0.999	0.241	38.25	0.941	62.45	0.829	0.941
298	61.25	67.39	0.229	0.042	0.998	0.389	44.89	0.952	68.14	1.124	0.926
323	65.44	73.64	0.286	0.334	0.995	0.526	53.12	0.966	72.98	1.536	0.937

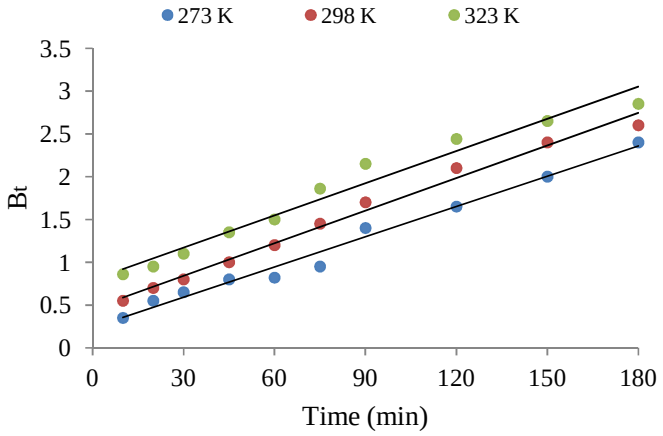

Fig. 9. Plot of B_t Versus t for the adsorption of CIP on HSAC at different temperatures

Table 4. Thermodynamic parameters for the adsorption of CIP on HSAC

T (K)	ΔG^0 (kJ/mol)	ΔH^0 (kJ/mol)	ΔS^0 (kJ/mol K)
273	−3.39		
298	−4.82	3.064	0.0261
323	−5.65		

The Freundlich isotherm model is valid for multilayer adsorption on a heterogeneous adsorbent surface with sites that have different energies of adsorption. The Freundlich model in linear form is presented by equation 11 [41]:

$$\text{Ln } q_e = \ln K_F + \frac{1}{n} \ln C_e \quad (11)$$

Where K_F (mg/g) is the constant related to the adsorption capacity and n is the empirical parameter related to the intensity of adsorption. The value of n varies with the heterogeneity of the adsorbent and for favorable adsorption process the value of n should be less than 10 and higher than unity. The values of K_F and 1/n are determined from the intercept and slope of linear plot of ln q_e versus ln C_e, respectively.

The obtained isothermal constants and the correlation coefficients are presented in Table 3. It is found that the adsorption of CIP on HSAC correlated well (R^2>0.995) with the Langmuir equation as compared to the Freundlich equation (R^2>0.94) under the studied concentration range. Therefore, the Langmuir isotherm fits better compared with the Freundlich isotherm in all conditions according to the correlation coefficients R^2. The maximum adsorption capacity (q_{max}) of CIP on HSAC was 61.25, 67.39, 73.64 mg/g at 273, 298 and 323 K, respectively and at the same temperatures q_e experimental was 57.26, 61.25 and 65.44 mg/g. The results showed (Table 3) that the q_{max} obtained from the Langmuir isotherm were in almost agreement with the experimental adsorption capacity values for this model.

Finally, the Dubinin–Radushkevich (D–R) isotherm is presented by equation 12 [42-44]:

$$\text{Ln } q_e = \ln q_m - K\varepsilon^2 \quad (12)$$

Where q_e and q_m have the same meaning as above, K is the parameter related to the adsorption energy. ε is the adsorption potential, defined by Polanyi as the free energy change required to move a molecule from bulk solution to the adsorption area. The polanyi potential varies with the concentration according to [45]:

$$\varepsilon = RT \ln \left(1+\frac{1}{C_e}\right) \quad (13)$$

Where R is the ideal gas constant and T is the temperature (K). The D–R constants are presented in Table 3 and indicating that CIP adsorption also obeys the D–R equation. The adsorption energy for CIP adsorption can be calculated by equation 14 [46,47]:

$$E=(-2K)^{-1/2} \quad (14)$$

The values of the adsorption energy were evaluated as 0.829, 1.124 and 1.536 kJ/mol at 273, 298 and 323 K, respectively, indicating that the values lie within the energy range of physical adsorption, i.e.,<8 KJ/mol.

3.6 Evaluation of Thermodynamic Parameters

The adsorption capacity increased with increase of the temperature, indicating that the adsorption is endothermic, which was further explained by evaluation of thermodynamic parameters. The thermodynamic parameters, including standard Gibbs free energy change (ΔG^0, kJ/mol), standard enthalpy change (ΔH^0, kJ/mol) and standard entropy change (ΔS^0, kJ/mol K) were calculated to gain further insights into the adsorption mechanism of CIP on HSAC. The thermodynamic parameters of adsorption are expressed by equations 15-17 [48-50]:

$$\Delta G^0 = -RT \ln K \quad (15)$$

$$\ln (K_L) = \frac{\Delta S^0}{R} - \frac{\Delta H^0}{RT} \quad (16)$$

$$\Delta G^0 = \Delta H - T \Delta S^0 \quad (17)$$

where R, T and K are the universal gas constant (8.314 J. K^{-1} mol^{-1}), the absolute temperature (K) and the distribution coefficient, respectively. Thermodynamic parameters were listed in Table 4. The negative values of ΔG^0 indicated the adsorptive performance of CIP on the HSAC were feasible and spontaneous. Furthermore, the absolute values of ΔG^0 decreased with the increased of temperature, indicating that the presence of an energy barrier at low temperature in the adsorption and the adsorption was favorable at high temperature [50]. The positive values of ΔH^0 confirmed the endothermic nature of the adsorption process, while the positive values of ΔS^0 suggested the randomness at the solid and solution interface was increasing during the adsorption process [51].

4. CONCLUSION

Isotherms, kinetic and thermodynamic studies were accomplished for the CIP removal using HSAC. The adsorption kinetic data were well described by the pseudo-second-order model at different temperatures. The equation of Weber and Morris was employed to evaluate the adsorption mechanism of CIP on the HSAC and the results indicated that both the intraparticle diffusion and the boundary layer diffusion control the adsorption process. The parameters were analysed using Langmuir, Freundlich and D–R adsorption isotherm and equilibrium data were well fitted to the Langmuir isotherm models. The enthalpy change (ΔH^0) for the adsorption of CIP onto HSAC signifies an endothermic adsorption. The ΔG^0 value is negative at all studied temperatures, inferring that, the adsorption of CIP onto HSAC will follow a spontaneous trend. The ΔG^0 value decreased when the temperature increased from 273 to 323 K, suggesting increase in adsorption of CIP with increasing temperature. The positive value of ΔS^0 suggests increased randomness at the solid-solution interface.

CONSENT

It is not applicable.

ETHICAL APPROVAL

It is not applicable.

ACKNOWLEDGEMENTS

The authors would like to acknowledge from Zahedan University of medical sciences for the support this study.

COMPETING INTERESTS

Authors have declared that no competing interests exist.

REFERENCES

1. Garoma T, Umamaheshwar SH, Mumper A. Removal of sulfadiazine, sulfamethizole, sulfamethoxazole, and sulfathiazole from aqueous solution by ozonation. Chemosphere. 2010;79:814-20.
2. Alexy R, Kumpel T, Kummerer K. Assessment of degradation of 18 antibiotics in the closed bottle test. Chemosphere. 2004;57:505–512.
3. Choi KJ, Kim SG, Kim SH. Removal of antibiotics by coagulation and granular activated carbon filtration. J. Hazard. Mater. 2008;151:38-43.
4. Balarak D, Mahdavi Y, Maleki A, Daraei H, Sadeghi S. Studies on the removal of amoxicillin by single walled carbon nanotubes. British Journal of Pharmaceutical Research. 2016;10(4):1-9.

5. Peng X, Hu F, Dai H, Xiong Q. Study of the adsorption mechanism of ciprofloxacin antibiotics onto graphitic ordered mesoporous carbons. Journal of the Taiwan Institute of Chemical Engineers. 2016;8:1–10.
6. Huang L, Wang M, Shi C, Huang J, Zhang B. Adsorption of tetracycline and ciprofloxacin on activated carbon prepared from lignin with H_3PO_4 activation. Desalination and Water Treatment. 2014; 52:2678-87.
7. Amini M, Khanavi M, Shafiee A. Simple high-performance liquid chromatographic method for determination of ciprofloxacin in human plasma. Iranian Journal of Pharmaceutical Research. 2004;2:99-101.
8. Dhafir T, Al-Heetimi A, Kadhum MAR, Alkhazrajy OS. Adsorption of ciprofloxacin hydrochloride from aqueous solution by Iraqi porcelinaite adsorbent. Journal of Al-Nahrain University. 2014;17(1):41-49.
9. Malakootian M, Balarak D, Mahdavi Y, Sadeghi SH, Amirmahani N. Removal of antibiotics from wastewater by *Azolla filiculoides*: Kinetic and equilibrium studies. International Journal of Analytical, Pharmaceutical and Biomedical Sciences. 2015;4(7):105-113.
10. Balarak D, Mostafapour FK, Joghataei A. Experimental and kinetic studies on penicillin G adsorption by lemna minor. British Journal of Pharmaceutical Research. 2016;9(5):1-10.
11. Xu L, Pan J, Dai J, Li X, Hang H, Cao Z, Yan Y. Preparation of thermal-responsive magnetic molecularly imprinted polymers for selective removal of antibiotics from aqueous solution. Journal of Hazardous Materials. 2012;233-234:48-56.
12. Su YF, Wang GB, Kuo DTF, Chang ML. Photoelectrocatalytic degradation of the antibiotic sulfamethoxazole using TiO2/ Tiphotoanode. Applied Catalysis B: Environmental. 2016;186:184-192.
13. Balarak D, Azarpira H, Mostafapour FK. Study of the adsorption mechanisms of cephalexin on to *Azolla filiculoides*. Der Pharma Chemica. 2016;8(10):114-121.
15. Zhang L, Song X, Liu X, Yang L, Pan F, Lv J. Studies on the removal of tetracycline by multi-walled carbon nanotubes. Chem. Eng. J. 2011;178:26-33.
16. Ahmed MJ, Theydan SK. Adsorption of cephalexin onto activated carbons from *Albizia lebbeck* seed pods by microwave-induced KOH and K_2CO_3 activations. Chemical Engineering Journal. 2012;211-212:200–7.
17. Balarak D, Mahdavi Y, Mostafapour FK. Application of alumina-coated carbon nanotubes in removal of tetracycline from aqueous solution. British Journal of Pharmaceutical Research. 2016;12(1):1-11.
18. Yu F, Li Y, Han S, Jie Ma J. Adsorptive removal of antibiotics from aqueous solution using carbon Materials. Chemosphere. 2016;153:365–385.
19. Aksu Z, Tunc O. Application of biosorption for penicillin G removal: Comparison with activated carbon. Process Biochemistry. 2005;40(2):831-47.
20. Putra EK, Pranowoa R, Sunarsob J, Indraswatia N, Ismadjia S. Performance of activated carbon and bentonite for adsorption of amoxicillin from wastewater: mechanisms, isotherms and kinetics. Water Res. 2009;43:2419-2430.
21. Dutta M, Dutta NN, Bhattachary KG. Aqueous phase adsorption of certain beta-lactam antibiotics onto polymeric resins and activated carbon. Separation and Purification Technology. 1999;16(3):213-24.
22. Nazari G, Abolghasemi H, Esmaieli M. Batch adsorption of cephalexin antibiotic from aqueous solution by walnut shell-based activated carbon. Journal of the Taiwan Institute of Chemical Engineers. 2015;11:1-9.
23. Carabineiro A, Thavorn-Amornsri T, Pereira F, Figueiredo L. Adsorption of ciprofloxacin on surface modified carbon materials. Water Res. 2011;45:4583-91.
24. Chih-Jen W, Zhaohui L, Wei-Teh J. Adsorption of ciprofloxacin on 2:1 dioctahedral clay minerals. Applied Clay Science. 2011;53:723-28.
25. Ibezim EC, Ofoefule SI, Ejeahalaka N, Orisakwe E. *In vitro* adsorption of ciprofloxacin on activated charcoal and Talc. Am J Ther. 1999;6(4):199-201.
26. Franceline R, Nicolas T, Michel D, Tibiriça GV, Claire G, Sílvia SG, Adriana RP, Elias F. Spray-dried chitosan-metal microparticles for ciprofloxacin adsorption Kinetic and equilibrium studies. Soft Matter. 2011;7:7304-12.
27. Peterson JW, Petrasky LJ, Seymourc MD, Burkharta RS, Schuilinga AB. Adsorption

and breakdown of penicillin antibiotic in the presence of titanium oxide nanoparticles in water. Chemosphere. 2012;87(8):911–7.
28. Muthanna JA, Theydanb SK. Adsorption of cephalexin onto activated carbons from *Albizia lebbeck* seed pods by microwave-induced KOH and K_2CO_3 activations. Chem Eng J. 2012;211:200–7.
29. Dutta M, Baruah R, Dutta N, Ghosh A. The adsorption of certain semi-synthetic cephalosporins on activated carbon. Colloids Surf A Physicochem Eng Asp. 1997;127:25-37.
30. Balarak D, Mostafapour FK. Canola residual as a biosorbent for antibiotic metronidazole removal. The Pharmaceutical and Chemical Journal. 2016;3(2):12-17.
31. Zazouli MA, Mahvi AH, Dobaradaran S, Barafrashtehpour M, Mahdavi Y, Balarak D. Adsorption of fluoride from aqueous solution by modified *Azolla filiculoides*. Fluoride. 2014;47(4):349-58.
32. Liu Z, Xie H, Zhang J, Zhang C. Sorption removal of cephalexin by HNO_3 and H_2O_2 oxidized activated carbons. Sci China Chem. 2012;55:1959–67.
33. Liu H, Liu W, Zhang J, Zhang C, Ren L, Li Y. Removal of cephalexin from aqueous solution by original and Cu(II)/Fe(III) impregnated activated carbons developed from lotus stalks kinetics and equilibrium studies. J Hazard Mater. 2011;185:1528–35.
34. Balarak D, Mostafapour FK. Batch equilibrium, kinetics and thermodynamics study of sulfamethoxazole antibiotics onto *Azolla filiculoides* as a novel biosorbent. British Journal of Pharmaceutical Research. 2016;13(2):1-14.
35. Yang J, Que K. Preparation of activated carbons from walnut shells via vacuum chemical activation and their application for methylene blue removal. Chem Eng J. 2010;165:209-17.
36. Diyanati RA, Yousefi Z, Cherati JY, Balarak D. The ability of *Azolla* and *Lemna* minor biomass for adsorption of phenol from aqueous solutions. J Mazandaran Uni Med Sci. 2013;23(106):17-23.
37. Balarak D, Bazrafshan E, Kord Mostafapour F. Equilibrium, kinetic studies on the adsorption of acid green 3(AG3) dye onto *Azolla filiculoides* as adosorbent. American Chemical Science Journal. 2016; 11(1):1-10.
38. Zazouli MA, Yazdani J, Balarak D, Ebrahimi M, Mahdavi Y. Removal acid blue 113 from aqueous solution by canola. Journal of Mazandaran University Medical Science. 2013;23(2):73-81.
39. Hameed BH. Evaluation of papaya seed as a novel non-conventional low-cost adsorbent for removal of methylene blue. J Hazard Mater. 2010;162:939-94.
40. Ponnusami V, Vikram S, Srivastava SN. Guava (*Psidium guajava*) leaf powder: Novel adsorbent for removal of methylene blue from aqueous solutions. J Hazard Mater. 2008;152:276–86.
41. Balarak D, Jaafari J, Hassani G, Mahdavi Y, Tyagi I, Agarwal S, Gupta VK. The use of low-cost adsorbent (Canola residues) for the adsorption of methylene blue from aqueous solution: Isotherm, kinetic and thermodynamic studies. Colloids and Interface Science Communications. Colloids and Interface Science Communications. 2015;7:16–19.
42. Rostamian R, Behnejad H. A comparative adsorption study of sulfamethoxazole onto graphene and graphene oxide nanosheets through equilibrium, kinetic and thermodynamic modeling. Process Safety and Environmental Protection. 2016;102: 20-29.
43. Balarak D, Mahdavi Y, Bazrafshan E, Mahvi AH, Esfandyari Y. Adsorption of fluoride from aqueous solutions by carbon nanotubes: Determination of equilibrium, kinetic and thermodynamic parameters. Flouride. 2016;49(1):35-42.
44. Chen WR, Huang CH. Adsorption and transformation of tetracycline antibiotics with aluminum oxide. Chemosphere. 2010; 79:779-785.
45. Adrianoa WS, Veredasb V, Santanab CC, Gonçalves LRB. Adsorption of amoxicillin on chitosan beads: Kinetics, equilibrium and validation of finite bath models. Biochemical Engineering Journal. 2005; 27(2):132-37.
46. Zazouli MA, Mahvi AH, Mahdavi Y, Balarak D. Isothermic and kinetic modeling of fluoride removal from water by means of the natural biosorbents sorghum and canola. Fluoride. 2015;48(1):15-22.
47. Balarak D. Kinetics, isotherm and thermodynamics studies on bisphenol a adsorption using barley husk. International Journal of Chem Tech Research. 2016; 9(5):681-690.

48. Erşan M, Bağd E. Investigation of kinetic and thermodynamic characteristics of removal of tetracycline with sponge like, tannin based cryogels. Colloids and Surfaces B: Biointerfaces. 2013;104:75-82.
50. Balarak D, Mahdavi Y, Bazrafshan E, Mahvi AH. Kinetic, isotherms and thermodynamic modeling for adsorption of acid blue 92 from aqueous solution by modified *Azolla filicoloides*. Fresenius Environmental Bulletin. 2016;25(5):1321-30.
51. Balarak D, Azarpira H. Rice husk as a biosorbent for antibiotic metronidazole removal: Isotherm studies and model validation. International Journal of Chem Tech Research. 2016;9(7):566-73.

Peer-review history:
The peer review history for this paper can be accessed here:
http://sciencedomain.org/review-history/16334